

## The Electronic Spectra of Aromatic Molecular Crystals. II. The Crystal Structure and Spectra of Perylene

By JIRO TANAKA

(Received March 27, 1963)

The electronic absorption spectra of aromatic molecular crystals have been investigated from several viewpoints in order to confirm the polarizations and the symmetry properties of excited states, and in order to discover the mechanism of electronic interactions in molecular crystals.<sup>1)</sup> In spite of the many experiments which have been reported hitherto, few have been concerned with the same molecule in different crystalline forms. Perylene has two crystalline forms; the first was shown by Donaldson, Robertson and White<sup>2)</sup> to have a dimeric structure, while a new form, herein reported, is monomeric and analogous to the structures of naphthalene and anthracene. The electronic spectra of the two crystalline forms has been studied, and it has been shown that the charge-transfer resonance interaction is very important, particularly in the dimeric crystal. The anomalous fluorescence of dimers of pyrene and naphthalene in a solution<sup>3)</sup> and of pyrene and other substances in the crystalline state<sup>4,5)</sup> have attracted attention; the present study provides an explanation of the mechanism of anomalous fluorescence.

**Crystal Structure.**—It is proposed to designate the previously-known form of perylene by  $\alpha$  and the new one by  $\beta$ . Crystals of both the  $\alpha$  and  $\beta$  forms have been obtained together from petroleum ether or benzene solutions, but they are easily distinguished from each other by their general appearance. The  $\alpha$  form is usually obtained as a rectangular, tabular, yellow crystal (monoclinic), while the  $\beta$  form is obtained as hexagonal, greenish-yellow prisms (monoclinic). The  $\beta$  form is transformed into  $\alpha$  at about 140°C. At and below room temperature, both forms are stable, and no transformation was found at lower temperatures.

X-Ray rotation and Weissenberg photographs show that the  $\beta$  form belongs to the  $P2_1/a$  space group and give the following crystal data:  $a =$

$11.27 \pm 0.03$ ,  $b = 5.88 \pm 0.02$ ,  $c = 9.65 \pm 0.03$  Å,  $\beta = 92.1 \pm 0.3^\circ$ ; absent spectra; ( $h0l$ ) when  $h$  is odd and ( $0k0$ ) when  $k$  is odd; space group,  $P2_1/a$  ( $C_{2h}^{2h}$ ); two molecules per unit cell; the center of the molecule is at the origin; volume of the unit cell,  $394.3$  Å<sup>3</sup>. It should be noted that the lattice constants are similar to those of the  $\alpha$  form except for  $b$ , which is about half of the  $\alpha$  form ( $\alpha$  has  $a = 11.35$ ,  $b = 10.87$ ,  $c = 10.31$  Å and  $\beta = 100.8^\circ$ ; space group  $P2_1/a$  with four molecules in the unit cell.<sup>2)</sup>

The crystal structure analysis has been carried out with the aid of  $a$  and  $b$  axes projection. The  $h0l$  and  $0kl$  reflections were recorded with a Weissenberg camera using  $CuK\alpha$  radiation. The multiple-film technique was used, and the intensity data were obtained by

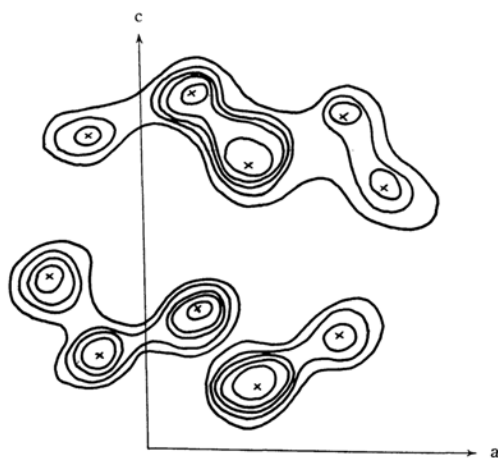


Fig. 1. Fourier map for the  $b$ -axis projection.

TABLE I

	$x$	$y$	$z$
$C_1$	0.092	0.170	0.044
$C_2$	0.169	0.323	0.117
$C_3$	0.214	0.331	0.270
$C_4$	0.177	0.190	0.344
$C_5$	0.091	0.020	0.292
$C_6$	0.044	-0.132	0.365
$C_7$	-0.050	-0.285	0.322
$C_8$	-0.083	-0.310	0.175
$C_9$	-0.037	-0.150	0.097
$C_{10}$	0.044	0.010	0.143

1) J. Tanaka, *Prog. Theoret. Physics*, Suppl. 12, 183 (1959).

2) D. M. Donaldson, J. M. Robertson and J. G. White, *Proc. Roy. Soc., A220*, 311 (1953).

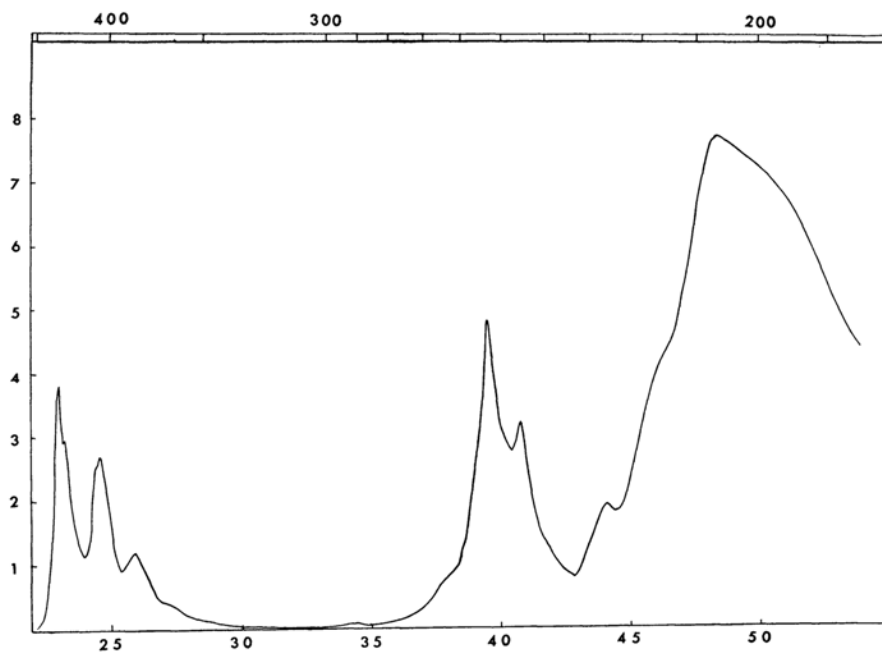
3) Th. Förster, Paper presented at the International Symposium on Molecular Structure and Molecular Spectroscopy, Tokyo, 1962.

4) J. Ferguson, *J. Chem. Phys.*, 28, 765 (1958).

5) B. Stevens, *Spectrochim. Acta*, 18, 439 (1956).

TABLE II. OBSERVED AND CALCULATED STRUCTURE FACTORS

Obs.	Calcd.	Obs.	Calcd.	Obs.	Calcd.	Obs.	Calcd.
001	80	404	5	601 $\bar{1}$	5	020	60
002	120	405	17	800	64	022	14
003	57	406	21	803	12	023	22
004	110	408	10	804	54	024	17
005	88	4010	8	805	50	027	31
006	9	40 $\bar{1}$	85	806	15	029	8
009	10	40 $\bar{2}$	28	80 $\bar{1}$	12	0211	5
200	114	40 $\bar{3}$	14	80 $\bar{2}$	8	032	5
201	63	40 $\bar{4}$	23	80 $\bar{3}$	7	033	5
202	40	40 $\bar{5}$	14	80 $\bar{4}$	11	036	8
203	34	40 $\bar{8}$	41	80 $\bar{5}$	26	038	9
204	131	40 $\bar{9}$	16	80 $\bar{9}$	7	040	14
205	11	40 $\bar{10}$	9	1002	3	041	6
206	30	600	34	1003	15	042	8
208	17	601	34	1004	37	043	8
209	29	602	14	120 $\bar{4}$	6	044	7
20 $\bar{1}$	116	605	12	011	7	047	18
20 $\bar{2}$	12	60 $\bar{1}$	8	012	23	049	2
20 $\bar{3}$	39	60 $\bar{2}$	7	013	6	054	6
20 $\bar{6}$	6	60 $\bar{4}$	65	014	41	055	7
20 $\bar{7}$	22	60 $\bar{5}$	26	015	43	060	42
20 $\bar{8}$	10	60 $\bar{6}$	12	016	12	061	11
20 $\bar{9}$	7	60 $\bar{7}$	22	017	14	062	9
400	6	60 $\bar{8}$	33	019	14	064	12
401	32	60 $\bar{9}$	46	0110	6	065	13
403	5	60 $\bar{10}$	5	0111	6		

Fig. 2. Absorption spectrum of perylene in *n*-heptane.Ordinate; molecular extinction coefficient (in units of  $10^4$ )Abscissa; lower, frequency (in  $10^3 \text{ cm}^{-1}$ ), upper, wavelength (in  $\text{m}\mu$ )

visual comparison with crystal-reflected calibration spots of known relative exposures. In the  $h0l$  zone, 69 intensities out of 140 were measured, and 41 out of 78 for  $0kl$ . The appropriate molecular orientation was deduced from the spectra of single crystals. A comparison with the spectrum showed that the directions of the long (L) and the short (M) axes of the molecules must be nearly the same in the two forms. Assuming that the tilts of the molecules on the axes are same in the two forms, the signs of the structure factors were determined; the first Fourier  $h0l$  projection showed the positions of all the carbon atoms. After a few cycles of refinement, the  $x$  and  $z$  parameters shown in Table I were obtained. The structure factors were calculated using the same temperature factor for all atoms,  $B=4.2$ , and at this stage of refinement,  $R$  (for the observed  $F_{h0l}$  reflection only) is 0.17. The calculated structure factors are compared in Table II with the observed values. The Fourier map for the  $b$  axis projection is shown in Fig. 1. The  $0kl$  Fourier projection did not show resolved atoms because of serious overlapping in this projection. Assuming that the molecule is planar and has nearly the same structure as in the  $\alpha$  form, the  $y$  parameters

shown in Table I may be derived and the structure factors  $F_{0kl}$  shown in Table II may be calculated. For the observed  $0kl$  reflections, the  $R$  factor is 0.27. Although, at this stage of refinement, the agreement between observed and calculated values is not sufficiently good to discuss the shape of the molecule, it seems reasonable to regard the  $\beta$  form as having a different structure from the  $\alpha$  form and as resembling the structures of naphthalene and anthracene. For convenience in the following discussion, we will regard the  $\alpha$  form as a

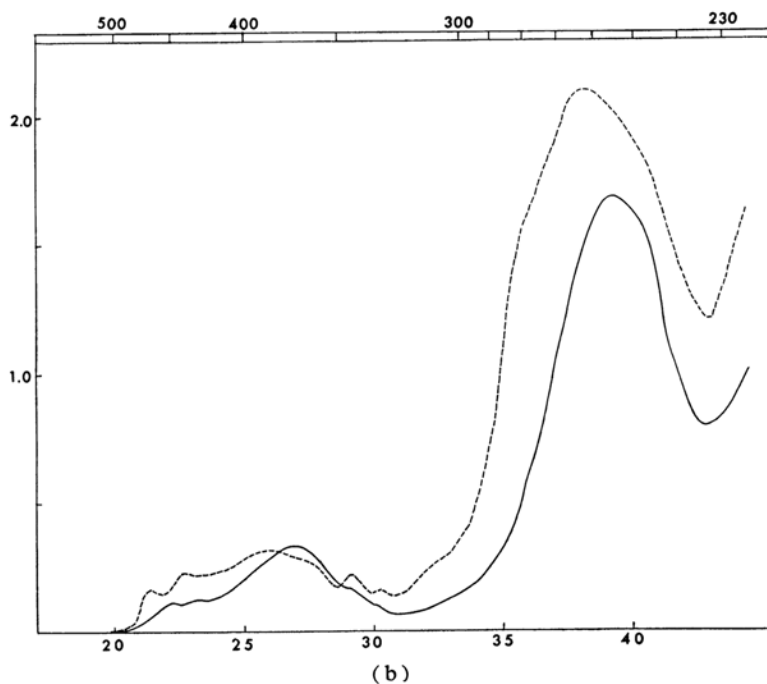
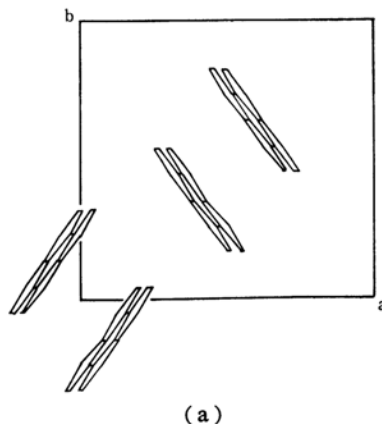


Fig. 3. (a) Projection of molecules in  $\alpha$  crystal form onto (001) plane. (b) Absorption spectrum of  $\alpha$  form through (001) plane.

— Light polarized parallel to  $a$ -axis

----- Light polarized parallel to  $b$ -axis

Ordinate; optical density

Abscissa; lower, frequency (in  $10^3 \text{ cm}^{-1}$ ), upper, wavelength (in  $m\mu$ )

dimer structure and the  $\beta$  form as a monomer structure of perylene.

**The Absorption Spectrum of the Perylene Crystals.**—The electronic absorption spectrum of perylene in the *n*-heptane solution shown in Fig. 2 has been measured by using a Cary Model 14 spectrophotometer. Three strong absorption bands are clearly seen at  $23050\text{ cm}^{-1}$  ( $f=0.33$ ), at  $39600\text{ cm}^{-1}$  ( $f=0.44$ ) and at  $48500\text{ cm}^{-1}$  ( $f=2.2$ ), and another weaker bands, at  $44200\text{ cm}^{-1}$ . Following the Hückel MO theory, the transition between the highest occupied and the lowest vacant orbital produces an excited state of symmetry  ${}^1B_{2u}$ , where the molecular symmetry is taken as  $D_{2h}$  and the two-fold axis is along the L-axis. This transition is allowed along the L-axis. The difference in orbital energy is  $0.647\beta$ , and the second one, of the same symmetry, is at  $1.347\beta$ , so that we can estimate roughly the energy of the first transition by the Pariser-Parr method<sup>6)</sup> by taking only the interaction between the highest occupied MO  $i$  and the lowest vacant MO  $j$  and by disregarding the

other orbitals. The excitation energy,  $\Delta E$ , is then given by;

$$\Delta E = 0.674\beta + K_{ij} \quad (1)$$

where  $K_{ij}$  represents the exchange electron integral between MO  $i$  and  $j$ ;

$$K_{ij} = \int \varphi_i^*(1) \varphi_j^*(2) 1/r_{12} \varphi_i(2) \varphi_j(1) d\tau_1 d\tau_2$$

The numerical calculation of  $\Delta E$ , carried out with  $\beta$  taken as  $-2.371\text{ eV}$ ,<sup>7)</sup> gives  $2.84\text{ eV}$ , the observed value being  $2.85\text{ eV}$ . Of course, this agreement occurs because of the cancellation of terms due to exchange integrals which

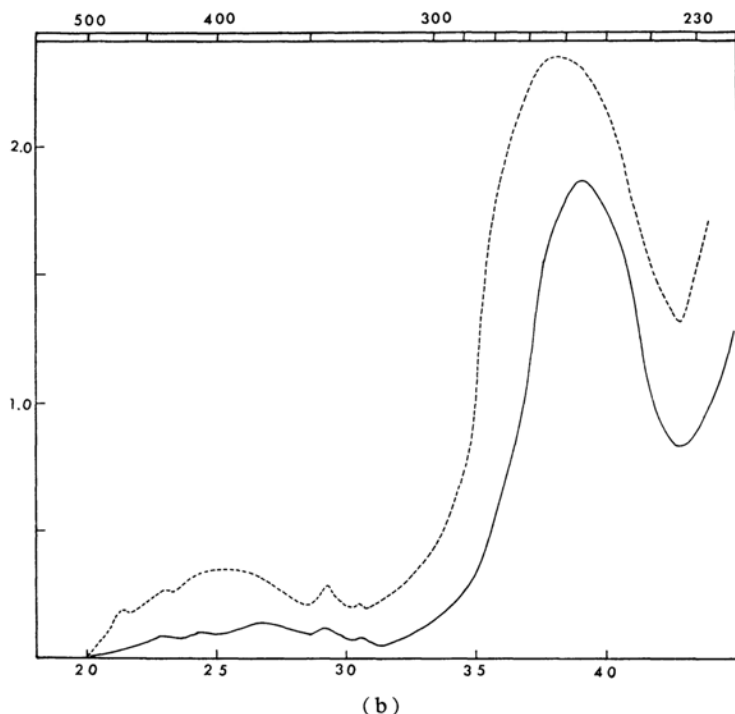
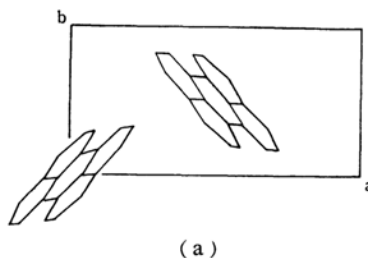


Fig. 4. (a) Projection of molecules in  $\beta$  crystal form onto (001) plane. (b) Absorption spectrum of  $\beta$  form through (001) plane.

— Light polarized parallel to a-axis

----- Light polarized parallel to b-axis

Ordinate; optical density

Abscissa; lower, frequency (in  $10^3\text{ cm}^{-1}$ ), upper, wavelength (in  $m\mu$ )

6) R. Pariser and R. G. Parr, *J. Chem. Phys.*, **21**, 466, 767 (1953).

7) R. Pariser, *ibid.*, **24**, 250 (1956).

TABLE III

Band (cm <sup>-1</sup> )	Polarization (direction of the transition moment)	Direction cosine to crystal axes		Calculated oscillator strength*		Calculated and observed dichroic ratio	
$\alpha$ Form		cos $\theta_a$	cos $\theta_b$	$a$	$b$	$a : b(\text{calcd.})$	$a : b(\text{obs.})$
23050	L-axis	0.117	0.014	0.0143	0.0002	71.5 : 1.0	0.82 : 1.0
39600	M-axis	0.618	0.783	0.535	0.856	1.0 : 1.60	1.0 : 1.46
$\beta$ Form							
23050	L-axis	0.343	0.044	0.122	0.002	61.0 : 1.0	0.35 : 1.0
39600	M-axis	0.615	0.771	0.526	0.829	1.0 : 1.57	1.0 : 1.25

\* The value of  $3f\cos^2\theta_{a,b}$  is presented, where  $f$  is the oscillator strength of the solution's absorption band. For 23050 cm<sup>-1</sup> band the values of  $\cos\theta_{a,b}$  of the L-axis polarization are used, and for the 39600 cm<sup>-1</sup> band, the M-axis values are used.

TABLE IV

Band of solution cm <sup>-1</sup>	$f$	Assignment	$\alpha$ Form				$\beta$ Form			
			Band in crystal		Splitting		Band in crystal		Splitting	
			$a$	$b$	(obs.)	(calcd.)	$a$	$b$	(obs.)	(calcd.)
23050	0.15	$^1B_{2u}$ (L-axis)	22200	21400	800	1020	22930	21370	1560	2360
24610	0.10		23150	22730	420	635	24390	23040	1350	1470
26000	0.07		25380	24750	630	450	26670	25000	1670	1180
—		charge transfer	27000	26450	550					
34500			29180	29180	0		29240	29240	0	
			30300	30300	0		30300	30300	0	
39600	0.44	$^1B_{3u}$ (M-axis)	39100	38600	500	-214	39100	38200	900	-2460
40860										
44200	0.15									
48500	2.17									

have been neglected and of the effect of configurational interaction with other higher excited states. However, it seems certain that the 23050 cm<sup>-1</sup> band corresponds to the  $^1B_{2u}$  excited state and is polarized along the L-axis. The 39600 cm<sup>-1</sup> band is presumably polarized along the short axis (M-axis), since the next higher level is often orthogonal to the first level.

The crystalline absorption spectra of both the  $\alpha$  and  $\beta$  forms presented in Figs. 3 and 4 have been obtained through the (001) plane by the method described in a previous paper.<sup>8,9</sup> The projection of molecules onto the (001) plane is also shown in Figs. 3 and 4. Hochstrasser<sup>9</sup> has discussed the spectrum of the  $\alpha$  form in the 20000~30000 cm<sup>-1</sup> region, but his labeling of the crystal axes seems to be mispolarized; his a-axis should be read as b and his b-axis as a. In the present study, all crystalline axes were determined by X-ray rotation photograph. Based on the oriented gas model, the intensities of the crystalline absorption bands can be predicted as in Table III. Re-

ferring to the values of the direction cosine in Table III, it can be seen that the intensity of the absorption band polarized along the L-axis should be far less than the M-axis polarized band in the (001) spectrum if the oscillator strengths are the same. The  $f$  values of the 23050 cm<sup>-1</sup> and 39600 cm<sup>-1</sup> bands are of the same order of magnitude, so it can be shown from the spectra (Figs. 3 and 4) that the 23050 cm<sup>-1</sup> band corresponds to the excited level of  $^1B_{2u}$  symmetry, while the 39600 cm<sup>-1</sup> band belongs to  $^1B_{3u}$  symmetry. The observed dichroic ratios for the 39600 cm<sup>-1</sup> band are in good agreement with the calculated values; hence the oriented gas model holds well for the 39600 cm<sup>-1</sup> band in both the  $\alpha$  and  $\beta$  forms.

Table IV lists all the observed band positions and assignments. The splitting of bands has been observed for 39600 cm<sup>-1</sup> band; values of 500 cm<sup>-1</sup> and 900 cm<sup>-1</sup> are recorded for the  $E_a-E_b$  splitting in the  $\alpha$  and  $\beta$  forms.

The calculation of the Davydov splitting has been carried out by the standard method, taking into consideration the dipole-dipole interaction of molecules within a 20 Å sphere.

8) J. Tanaka, This Bulletin, 36, 833 (1963).

9) R. Hochstrasser, Can. J. Chem., 39, 451 (1961).

For the  $\beta$  form, the two excited state wave functions  $\Psi^r$  and  $\Psi^s$ , which are active along the a and b axes respectively, are written as:

$$\begin{aligned}\Psi^r &= \frac{1}{\sqrt{2N}} \left( \sum_{j=1}^N \varphi'_{1j} - \sum_{i=1}^N \varphi'_{2i} \right) \\ \Psi^s &= \frac{1}{\sqrt{2N}} \left( \sum_{j=1}^N \varphi'_{1j} + \sum_{i=1}^N \varphi'_{2i} \right)\end{aligned}\quad (2)$$

where  $\varphi'_{1j}$  represents a crystal wave function in which a molecule on the 1jth site is excited and where  $\varphi'_{2i}$  denotes a crystal wave function in which the 2ith site molecule is excited. The summation over  $N$  means that the excitation moves through the  $2N$  molecules;  $i=1, 2, \dots, N, j=1, 2, \dots, N$ . The splitting between b and a axes ( $E_b - E_a$ ) may then be given by

$$\begin{aligned}E_b - E_a &= 2V_{12} \\ &= 2 \sum_{i=1}^N \int \varphi_1(1) \varphi'_1(1) H \varphi_2(2) \varphi'_{2i}(2) d\tau_1 d\tau_2\end{aligned}\quad (3)$$

where  $\varphi'_1(1)$  and  $\varphi'_{2i}(2)$  are the excited state wave functions of the 1st and 2ith molecules, and  $H$  is Hamiltonian of the system. The coordinates of transition dipoles chosen for the 1st and 2nd molecules are 1 (xyz) 2 ( $1/2-x, 1/2+y, \bar{z}$ ); they are related to each other by the screw axis rotation about the b-axis.

For the  $\alpha$  form, the excited states which belong to the  $B_u$  and  $A_u$  representation of the  $C_{2h}^s$  space group and which are active along the a- and b-axes respectively are written by:

$$\begin{aligned}\Psi^\zeta &= \frac{1}{\sqrt{4N}} \left( \sum_{i=1}^N \varphi'_{1i} - \sum_{j=1}^N \varphi'_{2j} - \sum_{k=1}^N \varphi'_{3k} + \sum_{l=1}^N \varphi'_{4l} \right) \\ \Psi^\epsilon &= \frac{1}{\sqrt{4N}} \left( \sum_{i=1}^N \varphi'_{1i} - \sum_{j=1}^N \varphi'_{2j} + \sum_{k=1}^N \varphi'_{3k} - \sum_{l=1}^N \varphi'_{4l} \right)\end{aligned}\quad (4)$$

where  $\varphi'_{1i}, \varphi'_{2j}, \varphi'_{3k}$ , and  $\varphi'_{4l}$  represent the crystal wave functions in which the 1i, 2j, 3k, and 4l molecules are excited. They are related to each other by the symmetry operation of the crystal. The coordinates of transition dipoles chosen are 1 (x, y, z), 2 ( $\bar{x}, \bar{y}, \bar{z}$ ), 3 ( $1/2-x, 1/2+y, \bar{z}$ ) and 4 ( $1/2+x, 1/2-y, z$ ). The excitation transfer matrix elements for  $\Psi^\zeta$  and  $\Psi^\epsilon$  are given by:

$$\begin{aligned}V^\zeta &= \frac{1}{4} (-V_{11} - V_{13} + V_{14} + V_{23} - V_{24} - V_{34}) \\ V^\epsilon &= \frac{1}{4} (-V_{11} + V_{13} - V_{14} - V_{23} + V_{24} - V_{34})\end{aligned}\quad (5)$$

the notation for  $V_{12}$  is given in Eq. 3. The splitting between a and b axes is given by:

$$E_a - E_b = V_{14} - V_{13}\quad (6)$$

The calculated energies  $V_{12}, V_{13}$  and  $V_{14}$ , using

the Hamiltonian for the dipole-dipole interaction only, are given in Table V.

The splittings calculated for the  $39600\text{ cm}^{-1}$  band are  $-214\text{ cm}^{-1}$  and  $-2460\text{ cm}^{-1}$  for the  $\alpha$  and  $\beta$  forms respectively, but the observed values are  $500\text{ cm}^{-1}$  and  $900\text{ cm}^{-1}$ . The calculated values do not agree even in sign for the two forms. Presumably the interaction with higher excited levels will be strong enough to change the energy level in the crystal.

In the region of the first absorption band near  $20000\sim 32000\text{ cm}^{-1}$ , we have found more important deviations from the oriented gas model based on the solution spectrum. First of all, we have noticed a broad band appearing in both the  $\alpha$  and the  $\beta$  forms instead of the sharp vibrational band in solution, although, even at room temperature, some vibrational structure can be seen. The Davydov splitting has been calculated assuming both the L-axis polarization and the weak interaction model of Simpson and Peterson,<sup>10)</sup> although the general pattern of the spectrum seems to be intermediate coupling. The results are listed in Table IV. It shows a general agreement between the observed and the calculated values, but the former is smaller than the latter. This discrepancy is attributed to the interaction with other excited states, particularly the charge transfer state, to the inadequacy of the dipole-dipole approximation, and to the over-estimation of the transition moment in crystal because a large hypochromism was observed for this band.

TABLE V

$\alpha$ Form		$V_{14}$	
$V_{13}$			
${}^1B_{2u}(L)$	${}^1B_{3u}(M)$	${}^1B_{2u}(L)$	${}^1B_{3u}(M)$
-802	-562	882	-768
$\beta$ Form			
$V_{12}$			
${}^1B_{2u}(L)$	${}^1B_{3u}(M)$		
-1840	1184		

All energies in  $\text{cm}^{-1}/\text{\AA}^2$ . The explicit form for  $V_{12}$  is, for example, given by:

$$V_{12} = -\frac{e^2}{R^3} \mu^2 \{ 2 \cos \theta_z \cos \theta_{z'} - \cos \theta_x \cos \theta_{x'} - \cos \theta_y \cos \theta_{y'} \}$$

where  $R$  is the distance between the centers of two transition moments,  $\mu$  is its magnitude ( $\text{\AA}$ ), and  $\cos \theta_z, \cos \theta_{z'}, \cos \theta_x, \cos \theta_{x'}, \cos \theta_y$  and  $\cos \theta_{y'}$  are the direction cosines of the transition moments on each molecule referred to the axis drawn between the two centers as the Z axis, with the X and Y axes orthogonal to the Z axis.

10) W. T. Simpson and D. L. Peterson, *J. Chem. Phys.*, **26**, 588 (1957).

In the  $\alpha$  form spectrum near 25000~28000  $\text{cm}^{-1}$ , we have found another absorption band, one which we have assigned to the charge transfer between molecules for the following reasons. First of all, this band is particularly apparent in the dimer form, in which the charge transfer interaction should be larger than in the monomer form. However, the intensity of this type of band cannot be expected to be large since in the ground-state crystal configuration, the molecules are separated by about 3.5 Å and since the electron overlap is relatively small. Therefore, this band will appear by borrowing intensity from the  $^1B_{2u}$ -allowed excited state by configurational mixing. Still, however, it has a different dichroic ratio ( $D_b:D_a$ ) to the first two absorption bands near 21000~23000  $\text{cm}^{-1}$ . The band is rather stronger along the a-axis than along the b-axis, which is another reason for assigning it to a different origin. The theoretical study of the electronic structure of the aromatic-excited dimer of perylene has recently been made by Murrell and Tanaka,<sup>11)</sup> who show that the perylene dimer has four excited singlet states in this region and that the allowed charge transfer band should appear at about 26600  $\text{cm}^{-1}$  (cf. Fig. 5 and the  $^1G \rightarrow ^1R_u$  transition at 3.5 Å). The observed band is at 26500~27000  $\text{cm}^{-1}$ ; hence, its assignment to the charge

transfer is supported by the theoretical treatment.

The direction of the transition moment of this charge transfer band is of interest when compared with that in other molecular complexes, where the direction is vertical to the aromatic ring.<sup>12)</sup> In the case of the aromatic dimer, the intensity is probably mainly due to the interaction with the allowed transition of the molecule, and the direction is along the molecular axis in the plane rather than vertical to it. The spectrum of the  $\alpha$  form shows that the band is stronger along the a-axis, where the molecular L-axis lies.

The splitting of the charge transfer band along the a and b axes is, though less definite, nearly 550  $\text{cm}^{-1}$ . This magnitude is so large that we must also consider the migration of the charge transfer state (the locally-ionized state) in the crystal. Although the charge transfer state will polarize the crystal and distort the lattice to some extent, its migration in the crystal introduces a new mechanism of photoconduction in aromatic crystals. By means of this mechanism, the locally-ionized state is considered to move rather easily, and its dissociation into electron and hole at an electrode surface will result in a transport of the electric charge. The band width of this state, or the excitation transfer matrix element between molecules, will be large than the usual band width of molecular orbitals in crystals; hence, the charge mobilities in molecular crystals will be increased.

The energy level of the charge transfer state for the monomer crystal ( $\beta$  form) can be estimated by the same method. Following the previous treatment,<sup>11)</sup> it is given by  $I-A-C$ , where  $I$  is the ionization potential of the molecule,  $A$ , its electron affinity, and  $C$  the electrostatic coulomb force between electron and hole. Introducing the numerical values of  $(I-A)=5.89$  eV. and  $C=2.07$  eV. for  $R=6.35$  Å separation leads to a charge transfer state at 3.82 eV. (30800  $\text{cm}^{-1}$ ), a state which could not be observed in the longer wavelength region and one which is hidden under the strong transition to the  $^1B_{3u}$  state.

Next we will discuss the hypochromism of the transition to the  $^1B_{2u}$ -excited state. It is seen from the projection in Figs. 3-4 that the L-axis is almost along the a-axis of the crystal. In this structure it is expected that absorption should appear only along the a-axis, not along the b-axis for the L-axis polarization band. However, the experimental results shows that the reverse is the case; it is rather stronger along the b-axis than along the a-axis. In

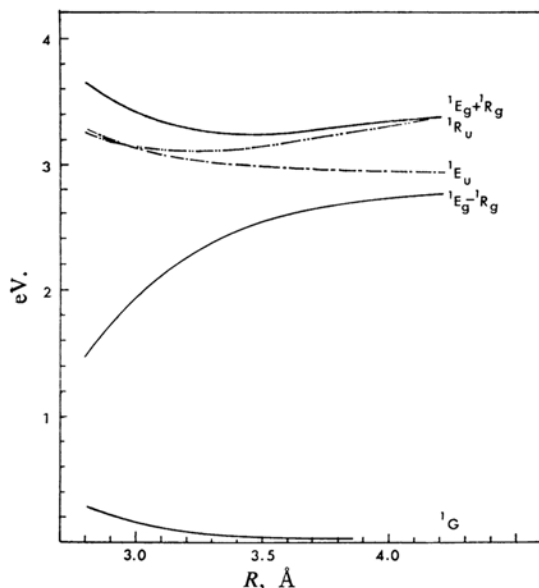


Fig. 5. Energy level diagram for the perylene dimer (only lower excited singlet levels having  $^1B_{2u}$  symmetry are shown).

Ordinate; energy in eV.

Abscissa, distance between two molecules

11) J. N. Murrell and J. Tanaka, *Mol. Phys.* (to be published); G. J. Hoijtink and E. Konijnenberg, *Z. phys. Chem.* (to be published).

12) K. Nakamoto, *J. Am. Chem. Soc.*, **74**, 1739 (1952).

TABLE VI. INTENSITY RATIOS OF THE  ${}^1B_{2u}$  BAND TO THE  ${}^1B_{3u}$  BAND

	Calculated		Observed	
	a-Axis ${}^1B_{2u} : {}^1B_{3u}$	b-Axis ${}^1B_{2u} : {}^1B_{3u}$	a-Axis ${}^1B_{2u} : {}^1B_{3u}$	b-Axis ${}^1B_{2u} : {}^1B_{3u}$
$\alpha$ Form	0.027 : 1.00	0.0002 : 1.00	0.20 : 1.00	0.17 : 1.00
$\beta$ Form	0.230 : 1.00	0.0025 : 1.00	0.11 : 1.00	0.21 : 1.00

Table VI the calculated and observed values of the intensity ratio of the  ${}^1B_{2u}$  band to the  ${}^1B_{3u}$  band are compared. It is seen that in the  $\beta$  form the observed a-axis absorption is greatly reduced while it is increased along the b-axis; in the  $\alpha$  form it increases in both directions, but to a greater extent along the b-axis. The increase along the b-axis may be explained by mixing with the next higher excited levels, but the decrease in the intensity, particularly along the a-axis, cannot be explained simply by the interaction with the allowed transition at higher energies. As has been mentioned previously, the transition to the charge transfer state has very little transition moment, so the interaction with this state may result in the hypochromism of the  ${}^1B_{2u}$  transition. This mechanism for hypochromism is reasonable if we consider the symmetry properties of these excited states. Both the  ${}^1B_{2u}$  and the charge transfer states involve the excitation of an electron from the highest occupied to the lowest vacant orbital of the same molecule or of the nearest neighbor molecule. Therefore, the symmetries of the molecular orbitals concerned are the same and the mixing of these states is allowed. For the  ${}^1B_{3u}$  excited state, however, no interaction with the lowest charge transfer state can be expected since the symmetry of the molecular orbital is different. Therefore, hypochromism, and other types of deviation from the oriented gas model, will be found only in the  ${}^1B_{2u}$  excited state and is, in fact, observed in the crystalline spectrum.

In the  $\alpha$  form the intensification of the charge transfer band and the decrease in the intensity of the  ${}^1B_{2u}$  transition caused by this interaction is observed along the a-axis. For the  $\beta$  form, however, because the charge transfer absorption is at a higher energy region and cannot be discerned, we found only a decrease in the intensity of the  ${}^1B_{2u}$  transition.\* In the crystal the interaction will take place not only between a pair of molecules in the dimer but through neighboring molecules, and the energy level of the charge transfer state will form a band, the excitation transfer will

occur more efficiently, and stronger hypochromism may be expected. The L-axis of the molecule, along which direction the interaction of molecular orbitals takes place, exactly coincides with the a-axis of both crystal forms, so that strong hypochromism is seen only along the a-axis. If the L-axis is not along the a-axis, but somewhere between the a- and b-axes, then hypochromism will be observed in both crystal directions.

Finally, it must be mentioned that at 29200 and 30500  $\text{cm}^{-1}$  there are new absorption bands which are not observed in solution. These bands will be of a different origin rather than vibrational progressions of the  ${}^1B_{2u}$  state because no splitting is observed in either the  $\alpha$  or  $\beta$  forms. A very weak absorption band in the solution spectrum at about 34500  $\text{cm}^{-1}$  is difficult to correlate without further information.

**The Fluorescence Spectrum of Perylene Crystals.**—The fluorescence spectra of both the  $\alpha$  and the  $\beta$  forms have been measured by the recording spectrofluorometer of Professor Makishima's laboratory.\* The machine consists of a mercury excitation lamp, a Kipp and Zonen double monochromator, and a

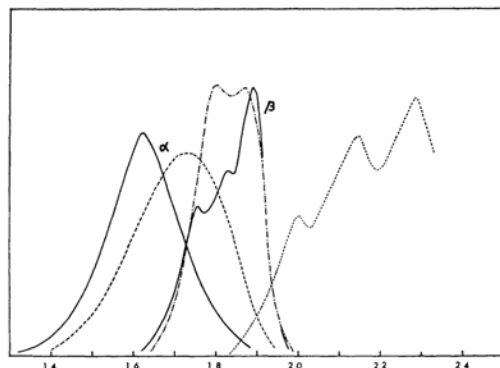


Fig. 6. Fluorescence spectrum of perylene.

----- solution in *n*-heptane  
 $\alpha$  form: — at 77°K  
 ----- at room temperature  
 $\beta$  form: — at 77°K  
 ----- at room temperature

Abcissa; frequency (in  $10^3 \text{ cm}^{-1}$ )

Ordinate; intensity (in arbitrary units)

\* The intensification of the charge transfer band along the a-axis, which will occur under the strong absorption band of the  ${}^1B_{3u}$  transition, will influence the dichroic ratio of the  ${}^1B_{3u}$  bands of the  $\beta$  form. In fact, the smaller observed value as compared with the calculated value or with the  $\alpha$  form can be explained on this basis.

\* The author wishes to express his thanks to Professors S. Makishima and S. Shionoya for the use of their spectrofluorometer.



photoelectric recording system. The spectra at room temperature and at the temperature of liquid nitrogen are shown in Fig. 6, together with the solution spectrum. It is most remarkable that the  $\beta$  form emits a green fluorescence at about  $18950\text{ cm}^{-1}$ , while the  $\alpha$  form glows yellow to red in the region of  $16000$  to  $17000\text{ cm}^{-1}$  and shifts markedly with the temperature. The green emission of the  $\beta$  form is regarded as a monomer emission of the crystal, while the red emission of the  $\alpha$  form is considered to be a dimer emission.

We will now discuss the origin of the dimer emission band from the theoretical point of view. First, a qualitative description of the charge transfer interaction, following Nagakura and Tanaka's one-electron approximation,<sup>13)</sup> will be given. Let us consider the interaction between the two ground state molecules. The wave function and the resonance energy for the charge transfer are given by:

$$\Psi = a\varphi_1 + b\theta_2$$

$$\Delta E = \frac{2\beta^2}{I_p - E_A}, \quad \beta = \int \varphi_1 H \theta_2 d\tau \quad (4)$$

where  $\varphi_1$  is the highest occupied orbital of the donor molecule and  $\theta_2$  is the lowest vacant orbital of the acceptor molecule. Because of the symmetry of  $\varphi_1$  and  $\theta_2$  (which are orthogonal if we take only the directly opposite interaction in the most symmetrical dimer), the resonance integral  $\beta$  will be very small; hence, no self-molecular complex can be formed between unexcited molecules, even if the relevant alternant hydrocarbon behaves as a good electron donor or acceptor in a mixed system. However, if one molecule is in the excited state, interaction takes place between  $\varphi_2$  and  $\theta_2$ , and the symmetry of the orbitals obviously favors a large interaction. Therefore, the molecule in the excited state (the  ${}^1B_{2u}$  excited state in the case of perylene) will be stabilized to a greater extent by a charge transfer complex formation with another unexcited molecule of the same species. It is well established that the absorption and fluorescence spectra of a molecular complex appear in completely different positions from those of the individual molecules and are mainly determined by the values of  $I_p$ ,  $E_A$  and  $\beta$  in Eq. 7. Hence, it is quite reasonable that the fluorescence of the excited dimer appears at longer wavelengths where there is no corresponding molecular transition. This is the qualitative explanation of the larger red shift of the excited dimer emission band.

Recently a more sophisticated quantitative treatment of this problem has been evolved

by Murrell and Tanaka, and by Hoijsink and Konijnenberg.<sup>11)</sup>

The calculation based on a non-overlap approximation which takes into account the exciton type interaction between the  ${}^1E_u$  and  ${}^1E_g$  states\* shows that the splitting of this type is not enough to explain the observed shift and gives the wrong order when compared to the observed shifts for naphthalene, pyrene and perylene. When electron overlap and delocalization are considered, and when the Hamiltonian matrix elements are evaluated, it is shown that the interaction between  ${}^1E_g$  and  ${}^1R_g$  produces a large splitting, with only a very slight splitting for the  ${}^1E_u$  and  ${}^1R_u$  states. Figure 5 shows the results of the calculation for this configurational interaction. It is seen that the  ${}^1E_g$ - ${}^1R_g$  state is most stabilized by electron delocalization between the molecules. Although the transition between the ground state and the  ${}^1E_g$ - ${}^1R_g$  state is forbidden by symmetry, long wave emission band of the dimer certainly corresponds to this transition because this is the only state which is greatly stabilized by charge resonance interaction. If the dimer is not completely symmetric, as in the crystal, the selection rule will not strictly forbid emission from the lowest singlet level. The stabilization of this level is greater, the shorter the molecular separation, so it is conceivable that the molecules will approach each other following the excitation of one of them. This means that a self-molecular complex has been formed between two molecules, of which one is in the excited state. Figure 5 shows that the red shift is mainly due to the stabilization of the  ${}^1E_g$ - ${}^1R_g$  state, but it is also due, to some extent, to the repulsion of the ground state at the closer molecular approach. The estimation of this distance is very difficult and necessarily involves guesswork, but a comparison of the observed and calculated values suggests a separation of  $3.1\sim 3.2\text{ \AA}$ . At this distance the stabilization of the  ${}^1E_g$ - ${}^1R_g$  state is about  $0.6\text{ eV}$ ., and the repulsion in the ground state is about  $0.1\text{ eV}$ .

\* The notations for the electronic configuration of the dimer, in which only the  ${}^1B_{2u}$  local excited state and the charge transfer state are considered, are as follows:

Configuration		
Ground	${}^1A^1A$	G
Excited Resonance	${}^1A^*{}^1A - {}^1A^1A^*$	${}^1E_u$
	${}^1A^*{}^1A + {}^1A^1A^*$	${}^1E_g$
Charge Resonance	${}^1(2A^*2A - 2A^*2A^*)$	${}^1R_u$
	${}^1(2A^*2A + 2A^*2A^*)$	${}^1R_g$

$${}^1A^1A = |\varphi_1\bar{\varphi}_1\theta_1\bar{\theta}_1|$$

$${}^1A^*{}^1A = \sqrt{1/2}(|\varphi_1\bar{\varphi}_2\theta_1\bar{\theta}_1| - |\varphi_1\bar{\varphi}_2\theta_1\bar{\theta}_1|)$$

$${}^1(2A^*2A) = \sqrt{1/2}(|\varphi_1\bar{\varphi}_2\theta_1\bar{\theta}_1| - |\varphi_1\bar{\varphi}_2\theta_1\bar{\theta}_1|)$$

where  $\varphi_1$ ,  $\theta_1$  and  $\varphi_2$ ,  $\theta_2$  are wave functions of the highest occupied and lowest vacant orbitals of each molecule and  ${}^1A^*$  is the lowest singlet excited state of  ${}^1B_{2u}$  symmetry.

13) S. Nagakura and J. Tanaka, *J. Chem. Phys.*, **22**, 236 (1954).

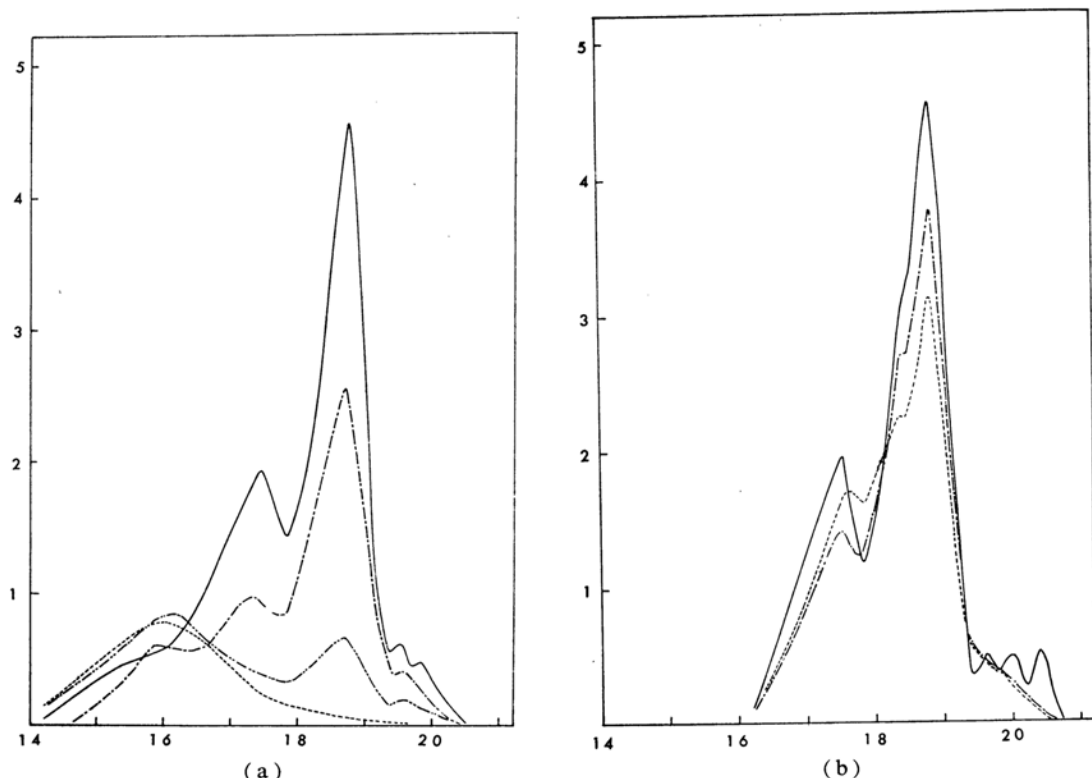


Fig. 7. Fluorescence spectrum of perylene crystals.

(a)  $\alpha$  Form  
 — at 4.2°K    - - - - at 33°K    - · - · - at 50°K    · · · · at 70°K

(b)  $\beta$  Form  
 — at 4.2°K    - - - - at 28°K    - · - · - at 80°K

Abscissa; frequency (in  $10^3 \text{ cm}^{-1}$ )

Ordinate; intensity of fluorescence (in arbitrary units, but with the same scale for different temperatures)

The dimer emission band shifts remarkably from  $17300 \text{ cm}^{-1}$  at room temperature to  $16250 \text{ cm}^{-1}$  at  $77^\circ\text{K}$ . This proves that the potential function of the excited state is rather shallow and that the population of the state is easily affected by the temperature.

The  $\beta$  form fluorescence shows a vibrational structure, but the  $\alpha$  form is structureless. This is explained by the potential curves of Fig. 5. The emission of the dimer form takes place between the excited state stabilized by charge transfer interaction and the ground state destabilized by repulsive interaction. Since the potential in the ground state is repulsive, discrete vibrational levels do not exist for this state and its population is continuous. Therefore, the dimer emission band has no vibrational structure.

Further experimental support for the idea of the movement of the molecule in the excited state in the  $\alpha$ -form crystal is given by the fluorescence measurement at the temperature

of liquid helium. The fluorescence spectra of  $\alpha$  and  $\beta$  forms between  $4.2$  to  $77^\circ\text{K}$  are shown in Figs. 7(a) and 7(b). The  $\beta$  form emission does not change in shape or position, but it does decrease in intensity with an increase in temperature; this is presumably due to the enhancement of the radiationless relaxation process at higher temperatures. In contrast to the small change of the  $\beta$  form emission, the yellow-red emission of the  $\alpha$  form changes to green at  $4.2^\circ\text{K}$  with no accompanying crystalline phase transition.\* By increasing the temperature to  $77^\circ\text{K}$ , the red emission appears again, and at intermediate temperatures both red and green emissions are observed.

\* The phase transformation from  $\beta$  to  $\alpha$  occurs at about  $140^\circ\text{C}$ . The  $\beta$  form is the metastable form at room temperature, and it is inconceivable that the  $\alpha \rightarrow \beta$  transformation occurs at a lower temperature. In fact, we can recover the  $\alpha$  crystal after its immersion in liquid helium without any of the damage to the original shape which would be expected if a phase transition had occurred.

Therefore, it is most probable that the dimer emission is prohibited at the temperature of liquid helium because the molecules are frozen out and cannot approach each other after excitation. In Fig. 5 we have considered only the energy of some molecular orbitals; however, the interaction between the other orbitals will give additional repulsion at a shorter molecular separation. The resultant potential function for the total system is as drawn in Fig. 8, in which the potential barrier appears at intermediate separation. Following the excitation of one molecule in the dimer with the nuclear separation fixed (the Franck-Condon principle) (process 1), it will relax into the lower of the singlet excited levels by radiationless process 2, cross the barrier (process 3) to the lowest of the singlet excited levels by changing the nuclear separation, and then emit at smaller energies (process 4). However, if the system is frozen out, the molecule has insufficient energy to surmount this potential

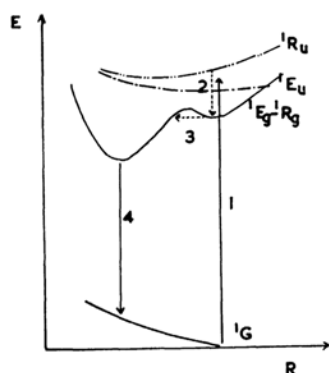
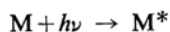


Fig. 8. Potential energy curve for the excited dimer including total repulsive energy.

barrier and hence remains at the larger molecular separation, with less stabilization of the excited energy level. In fact, the fluorescence spectrum of the  $\alpha$  form between 4~25°K shows only a green emission which is nearly the same as that of the  $\beta$  form, indicating that no stabilization of the excited state occurs because of the prohibition of the molecular movement. In the range between 25~40°K, the green emission is slowly quenched and the red emission appears instead, while above 40°K the quenching of the green and the appearance of the red occur more rapidly.

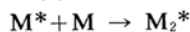
The rate process of the movement of the molecule to the closest position has been analyzed by the measurement of the intensity of the emission bands. We assume that the number of molecules frozen at the lattice sites is proportional to the intensity of the green emission; the decrease in the green emission intensity is considered to be proportional to the number of molecules which cross the barrier. The temperature dependence of the ratio at the red emission to the green emission is shown in Fig. 9, where the abscissa is  $1/T$  and the ordinate is the logarithm of the intensity ratio of the red to the green emission in an arbitrary unit. The kinetic scheme for the movement of the molecule after the excitation is given as follows:



(1) Molecules excited in the crystalline site



(2) Green emission, rate constant  $k_2$



(3) Excited dimer formation, rate constant  $k_3$

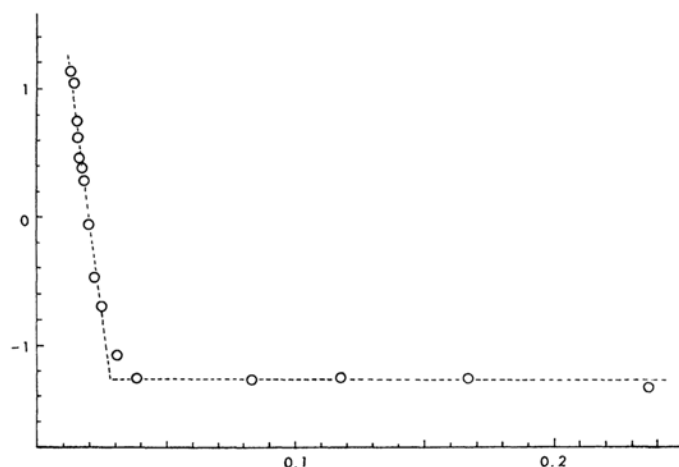
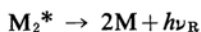


Fig. 9. Change in intensity ratio of red to green emission of the  $\alpha$  form crystal with temperature.

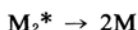
TABLE VII

	Solution			$\beta$ Form			$\alpha$ Form at 4.2°K		
	Abs.	Emis.	Shift	Abs.	Emis.	Shift	Abs.	Emis.	Shift
1st	23050	22800	250	21370	18880	2490	21400	18700	2700
2nd	24700	21500		22990	18400		22800		
3rd	26000	20000		25830	17550		25060	17420	

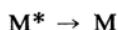
The band positions are expressed in wave numbers. The crystalline absorption is the mean value for the a- and b-axes.



- (4) Red emission from an excited dimer,  $k_4$



- (5) Radiationless deactivation of an excited dimer,  $k_5$



- (6) Radiationless deactivation of an excited monomer,  $k_6$

The molecule in the crystal is constantly illuminated; hence, the concentration of  $M^*$  in 1 is assumed to be constant. At the lower temperature, between 4.2 to 25°K, no appreciable decrease in the green emission is observed, so process 2 predominates with the natural emission coefficient of  $k_2$ . The numerical value of  $k_2$  is estimated from the absorption oscillator strength,  $f$ , by the use of the following relation:<sup>14)</sup>

$$k_2 = \frac{1}{1.5} \frac{g_1}{g_u} f \nu^2 = 1.2 \times 10^8 / \text{sec.} \quad (10)$$

where  $g_1$  and  $g_u$  are the spin multiplicity of the lower and upper states and  $\nu$  is the absorption frequency in wave numbers.

The intensities of the green and the red emission bands are given by

$$I_G = \frac{k_2 [M^*]}{k_2 + k_6}, \quad I_R = k_4 [M_2^*] = \frac{k_4}{k_4 + k_5} \cdot k_3 [M^*] \quad (11)$$

where  $[M^*]$  and  $[M_2^*]$  denote the concentration of the monomer and dimer molecules excited. The intensity ratio of the red to the green emission is given by

$$\begin{aligned} \frac{I_R}{I_G} &= \frac{k_4 [M_2^*]}{k_2 [M^*]} = \frac{k_4 k_3 (k_2 + k_6)}{k_2 (k_4 + k_5)} \\ &= \frac{k_4 (k_2 + k_6)}{k_2 (k_4 + k_5)} A_3 e^{-h\nu/kT} \end{aligned} \quad (12)$$

where  $k_3 = A_3 e^{-h\nu/kT}$ .

It follows that if we take the logarithm of

$I_R/I_G$  in the ordinate and  $1/T$  in the abscissa, we are able to estimate the activation energy of process 3. Figure 9 shows this relationship, the activation energy obtained from the slope between 40~80°K is  $\nu = 285 \text{ cm}^{-1}$ . This energy corresponds to the potential barrier in Fig. 8. At higher temperatures, most excited molecules go to the lowest state and emit a red fluorescence. The natural emission coefficient,  $k_4$ , estimated from comparison of the intensities of the red and green emission bands, gives  $f = 0.089$ . This fairly large value suggests a dipole-allowed transition, which is possible if the structure of the dimer is not completely symmetric and if the emission is not symmetry-forbidden.

The polarization of the dimer emission has been measured and the intensity was nearly the same in the a- and b-axes directions. However, the direction of the transition moment of the dimer emission band will not be discussed further, for we do not know the orientation of the excited molecule in the crystal.

Summarizing the above discussion, the mechanism of the red (dimer) emission is as follows:

After the excitation of one molecule of the dimer pair, the charge transfer resonance interaction taking place is larger at the shorter molecular separation, so the molecules approach each other and the excited dimer is formed. The emission from this stabilized state to the repulsive ground state appears at longer wavelengths. At very low temperatures, the motion of the molecule is inhibited and no stabilization by the excited-dimer formation can occur.

The present phenomenon somewhat resembles the quenching of the impurity fluorescence at very low temperatures.<sup>15)</sup> However, the mechanism of the emission is quite different, since the impurity fluorescence occurs by exciton migration to an impurity site, coupled with lattice vibrations, whereas the present phenomenon takes place by the movement of the molecule itself at each site in the crystal where a molecule is excited.

The emission of the  $\beta$  form appears at about

14) G. N. Lewis and M. Kasha, *J. Am. Chem. Soc.*, **66**, 2100 (1944).

15) Y. Kanda and H. Sponer, *J. Chem. Phys.*, **29**, 798 (1958); L. E. Lyons and J. W. White, *ibid.*, **29**, 447 (1958); K. Gschwendtner and H. C. Wolf, *Naturwiss.*, **48**, 42 (1961).

18880  $\text{cm}^{-1}$ ; its vibrational progressions are tabulated in Table VII, together with those for the solution and  $\alpha$ -form emissions. The  $\beta$ -form emission does not change position when the temperature is changed from 77 to 4.2°K. When the shifts of the first peak of the fluorescence from the first peak in the absorption is compared for the  $\beta$  form and for the solution, it is seen that a larger shift occurs in the  $\beta$ -form emission. The explanation for this stabilization of the excited state must be sought in such interaction as the charge transfer, but it is rather strange that the  $\beta$ -form and the  $\alpha$ -form emissions at the temperature of liquid helium do not differ greatly. In fact, the first peak position differs by only about 180  $\text{cm}^{-1}$ ; the shift from the absorption peak is 2700  $\text{cm}^{-1}$  for the  $\alpha$  form and 2490  $\text{cm}^{-1}$  for the  $\beta$  form, and the structure of the vibrational progression is certainly different. In view of the greater dependence of the charge-transfer resonance interaction on the nuclear separation, it is rather difficult to explain the almost identical emission bands from the different crystalline forms at low temperatures, but experiments show that the difference is rather small. The small peaks of the  $\beta$ -form emission near 20000  $\text{cm}^{-1}$  are due to surface states.

As a result of the observation of a green emission from the  $\beta$  and  $\alpha$  forms at the temperature of liquid helium, an alternative explanation for the observation by Hochstrasser<sup>16)</sup> of perylene-pyrene charge transfer fluorescence can be given. Of course, the possibility of charge-transfer resonance interaction between perylene-pyrene cannot be ruled out, but it should certainly be smaller than in the cases of perylene-perylene or pyrene-pyrene because the molecular orbitals concerned are of different types. The emission at 5250 Å of perylene in pyrene is almost identical with the  $\beta$ -form emission; therefore, it should be interpreted as a monomer emission of perylene in pyrene crystal.

### Summary

A new crystalline form of perylene has been found and its crystal structure has been determined by the two-dimensional X-ray diffraction method. The new form is monomeric, while the previously known form has a dimeric structure. The electronic absorption and fluorescence spectra of both forms have been measured; on the basis of these data, an assignment is proposed for the observed transitions. Although the fluorescence spectrum of the monomer form shows a small shift, that of the dimer form shows a larger shift than would be expected from the absorption spectrum. This is explained as a stabilization of the lowest excited singlet state by a charge-transfer resonance interaction between the molecules in a pair. Because this stabilization increases as the distance between two molecules decreases, it is suggested that the molecules in a pair approach each other after excitation. At the liquid helium temperature the motion of molecules in the crystal will be frozen out, the larger stabilization of the excited level cannot occur, and the green emission which is characteristic of the monomer form is observed from the dimer form. The rate process of the molecular motion at lower temperatures has been analyzed.

The author would like to express his thanks to Professor Saburo Nagakura for his continued encouragement of this work and to Professor Yoshihiko Saito and Mr. Hazime Iwasaki for their kind advice on crystal structure analysis. The author would also like to thank to Dr. John N. Murrell for discussions and hospitality during his stay in Sheffield. He also wishes to thank Dr. Brian Stevens of Sheffield University and Dr. Stephen C. Wallwork of Nottingham University for their criticism of the manuscript.

*The Institute for Solid State Physics  
The University of Tokyo  
Azabu, Tokyo*

16) R. Hochstrasser, *J. Chem. Phys.*, **36**, 1099 (1962).